frontiers in Ecology and Evolution

TYPE Original Research
PUBLISHED 12 August 2026
DOI 10.3389/fevo.2026.1889939

OPEN ACCESS

EDITED BY
Gerardo Carbot-Chanona,
Secretaría de Medio Ambiente e Historia Natural, Mexico

REVIEWED BY
Rémi Allemand,
Muséum National d'Histoire Naturelle, France
Serjoscha Evers,
Bavarian Natural History Collections, Germany

*CORRESPONDENCE
Adán Pérez-García
a.perez.garcia@ccia.uned.es

RECEIVED 24 May 2026
REVISED 21 July 2026
ACCEPTED 23 July 2026
PUBLISHED 12 August 2026

CITATION
Martín-Jiménez M and Pérez-García A (2026) Neuroanatomical study and ecological implications of the Maastrichtian pleurodiran bothremydid turtle *Zolhafah bella*. *Front. Ecol. Evol.* 14:1889939. doi: 10.3389/fevo.2026.1889939

Neuroanatomical study and ecological implications of the Maastrichtian pleurodiran bothremydid turtle *Zolhafah bella*

Marcos Martín-Jiménez and Adán Pérez-García*

Grupo de Biología Evolutiva, Facultad de Ciencias, UNED, Madrid, Spain

Bothremydidae was a succesful clade of pleurodiran turtles recognized from the Lower Cretaceous to at least the Eocene. This group included freshwater taxa (i.e., the members of Cearachelyini and most of Bothremydini) but also others recognized as littoral or even pelagic forms (i.e., Taphrosphyini and Nigeremydini). The Bothremydini *Zolhafah bella* was identified from the Maastrichtian of Egypt, only a skull being indisputably attributable to it. It was recovered from coastal sediments so that a marine way of life was inferred for it. The detailed external and internal anatomical analysis of the holotype of this species is performed here, from the three-dimensional models obtained from CT scan images, so that knowledge about its anatomy is increased. In addition, the study of neuroanatomical structures, nerve and vascular canals included into the endocranial and labyrinth cavities, is performed for the first time for the species, increasing the relatively scarce neuroanatomical information available for Bothremydidae. The anatomical and neuroanatomical comparisons between *Zolhafah bella* and other freshwater and marine bothremydids, including representatives of all lineages of this clade (i.e., Cearachelyini, Bothremydini, Nigeremydini, and Taphrosphyini), provide direct evidence to support a marine way of life for the species.

KEYWORDS
Bothremydidae, Egypt, neuroanatomy, pleurodira, Upper Cretaceous

1 Introduction

Bothremydidae was a successful clade of pleurodiran turtles recognized from the Early Cretaceous (Albian) to at least the Eocene, probably surviving until the Miocene, and having inhabited most of the continents in both the northern and southern hemispheres (Lapparent de Broin, 2000; Gaffney et al., 2006; Pérez-García, 2016a, b, 2018; Maniel et al., 2021). Despite some representatives being identified as freshwater forms (i.e., Cearachelyini and most species of Bothremydini; Gaffney et al., 2006; Pérez-García et al., 2012; Maniel et al., 2021), some taxa were suggested as coastal (i.e., some Bothremydini and Taphrosphyini) or even as pelagic turtles (i.e., Nigeremydini) (Lapparent de Broin and Werner, 1998; Gaffney et al., 2006; Cadena et al., 2012; Lapparent de Broin et al., 2021; Pérez-García, 2023; Martín-Jiménez and Pérez-García, 2025a). Most of these environmental implications were suggested based on the sedimentary environments where the fossils of these species were identified. However, the results of some adaptations to marine environments were identified

in some cranial features of these pleurodires, high skulls being suggested as related to short necks and reduced head retraction, as occurs in extant marine cryptodiran turtles (Werneburg et al., 2015; Hermanson et al., 2022; Ferreira et al., 2023). The possession of lacrimal glands to excrete the excess of salt observed in extant sea turtles (Schmidt-Nielsen and Fange, 1958; Hudson and Lutz, 1986; Marshall and Cooper, 1988; Wyneken, 2001) had been also suggested for Nigeremydini (Martín-Jiménez and Pérez-García, 2025a). The presence of large nasal openings has been evidenced for marine bothremydids, being proposed as a likely adaptation to that environment (Gaffney et al., 2006; Martín-Jiménez and Pérez-García, 2025a). However, large nasal cavities have been observed in both stem and cryptodiran tortoises, convergent to marine bothremydids, but in this case the size of the cavities has been interpreted as an adaptation to terrestrial and even arid environments (Paulina-Carabajal et al., 2017; Lautenschlager et al., 2018). In addition some neuroanatomical features, reflected in the endosseous labyrinth and the nasal cavity, have been identified as adaptations to a marine lifestyle (Parsons, 1959; Schwenk, 2008; Neenan et al., 2017).

Zolhafah bella Lapparent de Broin and Werner, 1998 was a bothremydid turtle identified by a single skull from the Maastrichtian Dakhla Formation of Egypt. The holotype of this member of Bothremydini comes from the Ammonite Hill member, deposited in a near shore marine environment (see Lapparent de Broin and Werner, 1998, and references therein). Numerous remains of littoral and pelagic animals were identified from these sediments including bony fishes, elasmobranchs and sea reptiles as plesiosaurs, mosasaurs, remains of the Bothremydidae Taphrosphyini of uncertain systematic attribution and the Bothremydidae Nigeremydini *Arenila krebsi* Lapparent de Broin and Werner, 1998. In this context, *Zolhafah bella* has been interpreted as a probable marine form, which has not been evaluated considering its anatomical and/or neuroanatomical characteristics. This taxon is identified as a member of Bothremydini (e.g., Gaffney et al., 2006; Pérez-García, 2016a, b), a lineage for which both freshwater forms and inhabitants of marine environments are known (Gaffney et al., 2006; Cadena et al., 2012; Pérez-García, 2016a, b). A detailed neuroanatomical study of this Egyptian species is presented here for the first time. Furthermore, knowledge of its cranial bone anatomy is improved. As a result, direct evidence regarding the marine lifestyle of this poorly known species is provided for the first time.

Institutional abbreviations: AMNH, American Museum of Natural History, New York, United States; FMNH, Field Museum of Natural History, Illinois, United States; GBE, Palaeontological Collection of the Grupo de Biología Evolutiva, Universidad Nacional de Educación a Distancia, Madrid, Spain; MB.R, Museum für Naturkunde, Berlin, Germany; MNHN.F, Palaeontology Collection, Muséum national d'Histoire naturelle, Paris, France; NHMUK, Natural History Museum, London, United Kingdom; TUB, Technische Universität Berlin, Berlin, Germany; YPM PU, Yale Peabody Museum, Princeton University collection, New Haven, United States.

Anatomical abbreviations: apo, antrum postoticum; asc, anterior semicircular canal; cas, canalis alveolaris superior; bo, basioccipital; bs, basisphenoid; cc, crus communis; ccb, canalis caroticus basisphenoidalis; ccv, canalis cavernosus; cer, cerebral hemispheres; cio, canalis infraorbitalis; clp, clinoid process; cprnv, canalis pro ramo nervi vidiani; cr, cartilaginous rider; cst, canalis stapedio-temporalis; ecc, endocranial cavity; eo, exoccipital; faca, foramen anterius canalis abducentis; faccb, foramen anterius canalis carotici basisphenoidalis; faf, fossa acustico-facialis; fcio, foramen canalis infraorbitalis; fcti, foramen chorda tympani inferius; fja, foramen jugulare anterius; fjp, foramen jugulare posterius; fm, foramen magnum; fnh, foramen nervi hypoglossi; fnt, foramen nervi trigemini; fpcci, foramen posterius canalis carotici interni; fpo, fenestra postotica; fpp, foramen palatinum posterior; fr, frontal; fst, foramen stapedio-temporalis; hyo, hyomandibular branch of facial nerve; I, olfactory nerve; ica, incisura columella auris; ima, inframaxillary artery; ioa, infraorbitary artery; ju, jugal; lc, labyrinthic cavity; lsc, lateral semicircular canal; mx, maxilla; mxp, maxillary pit; nc, nasal cavity; nop, nasal opening; npd, nasopharyngeal duct; ob, olfactory bulbs; olfd, olfactory duct; op, opisthotic; pa, parietal; pal, palatine; pf, prefrontal; pit, pituitary fossa; pm, premaxilla; pna, posterior nasal artery; pr, prootic; psc, posterior semicircular canal; pt, pterygoid; qu, quadrate; rbs, rostrum basisphenoidale; scv, sulcus cavernosus; sma, supramaxillary artery; so, supraoccipital; spp, sulus palatino-pterygoideus; V, trigeminal nerve; VI, abducens nerve; VII, facial nerve; VIII, vestibulocochlear nerve; vo, vomer; XII, hypoglossal nerve.

2 Materials and methods

The neuroanatomical analysis of the bothremydid *Zolhafah bella* performed here is based on the holotype and only known specimen of the species, TUB Vb-173. This fossil is housed in the Museum für Naturkunde (Berlin, Germany) with the number of collection MB.R. 2097. Most of the skull is preserved, but the right and left cheek bones (i.e., quadratojugals, part of jugals, and the anterior portion of the quadrates), the lateral walls of the endocranial cavity (sensu Ferreira et al., 2023), the postorbitals, and the occipital condyle are absent. In addition, some regions of the skull are eroded. The holotype of *Zolhafah bella* was presented and described by Lapparent de Broin and Werner (1998). Subsequently, Gaffney et al. (2006) reinterpreted some anatomical details. Therefore, detailed anatomical information about this specimen is available in the literature.

TUB Vb-173 was scanned at the Micro-CT Laboratory of the Museum für Naturkunde using a Phoenix Nanotom S X-ray Tomograph, with a voltage of 225 kV, a current of 110 μA, and 2,000 projections over 360°. The result of the scanning is the obtaining of 2,850 images in.dicom format with a resolution of 35 μm. Due to the large size of the files, the images were converted to.jpg format using the software ImageJ 1.50i (NIH, USA), and the images in which the fossil was not represented were removed, 1,561 files being considered. The segmentation of the modified images and the generation of virtual models of the skull, the right side and the medial bones, and the neuroanatomical structures, were carried out with the tools of the software Avizo 7.1 (VSG, Germany). Due to

a computational limitation of the workstation, the files obtained were processed into seven packages of 200 images and one more of 161. Three-dimensional meshes of both the osseous and the neuroanatomical elements were generated. The final models were obtained from the merge of the meshes generated from the packages, using tools of the Geomagic Studio 2014.3.0 software (3D Systems Corporation, USA). The 3D models were exported as .stl files. The linear and angular measurements of the inner cavities (i.e., endocranial, nasal, and labyrinths) and the carotid canals were performed using the tools of Avizo 7.1, and the volumetric ones were obtained using the software Geomagic Studio 2014.3.0. Bidimensional images of both the skull and the inner cavities were achieved by the rendering tools of Avizo 7.1, and the figures were generated using Adobe Photoshop CS6 13.0.

The three-dimensional models of the skull and the virtually isolated bones were compared with the description of Lapparent de Broin and Werner (1998) and Gaffney et al. (2006) in order to check if any interpretation should be amended or confirmed if it was raised as doubtful. The information of the neuroanatomical elements of *Zolhafah bella* has been compared with those of all other bothremydids for which available neuroanatomical reconstructions based on CT methodology. In this sense, the previously documented complete neuroanatomical studies of bothremydids are those of the Moroccan Cenomanian Cearachelyini *Galianemys whitei* Gaffney et al., 2002 (MNHN MRS 2098) and *Galianemys emringeri* Gaffney et al., 2002 (MNHN MRS 3105) (Martín-Jiménez and Pérez-García, 2022); the specimen MNHN.F.SPP34 of the Bothremydini *Tartaruscola teodorii* Pérez-García, 2016a, from the Eocene of France (Martín-Jiménez and Pérez-García, 2021); the holotype and only known specimen of the Nigeremydini *Azzabaremys moragjonesi* Gaffney et al., 2001, NHMUK R16370, from the Maastrichtian of Mali (Martín-Jiménez and Pérez-García, 2025a); and the specimen GBE-450 of the Taphrosphyini *Taphrosphys ippolitoi* Gaffney et al., 2006, from the Paleocene of Morocco (Martín-Jiménez and Pérez-García, 2025b). In addition, some neuroanatomical elements of other bothremydids were described and/or figured, as is the case of the endocranial cavity of the specimen AMNH 30008 of the Taphrosphyini *Phosphatochelys tedfordi* Gaffney and Tong, 2003, from the Eocene of Morocco (Hermanson et al., 2020); the facial and carotid canals of the specimen AMNH 29987 of the Cearachelyini *Galianemys whitei*, of the specimen AMNH 30569 of the Moroccan Eocene Taphrosphyini *Ummulisani rutgersensis* Gaffney et al., 2006, and of the individual AMNH 30043 of the Moroccan Eocene Taphrosphyini *Labrostochelys galkini* Gaffney et al., 2006 (Hermanson et al., 2020); and the labyrinth of the specimen AMNH 30234 of the Bothremydini *Bothremys maghrebiana* Gaffney et al., 2006, from the Paleocene of Morocco (Hermanson et al., 2020), and the previously indicated specimens of Taphrosphyini *Ummulisani rutgersensis* and *Phosphatochelys tedfordi* (Evers et al., 2022). In addition, the latex models of the endocasts of the North American Upper Cretaceous Bothremydini *Bothremys cooki* (Leidy, 1865), generated from the holotype AMNH 2521, and *Chedighaii barberi* (Schmidt, 1940), obtained from the specimen FMNH PR 247 (Gaffney and Zangerl, 1968), and the natural endocast of the specimen YPM PU 12951, identified as *Chedighaii* sp (Gaffney, 1977), were also compared with the virtual model of *Zolhafah bella* obtained in the present work.

3 Results

3.1 Systematic palaeontology

Testudines Batsch, 1788

Pleurodira Cope, 1864

Pelomedusoides Cope, 1868

Podocnemidoidea Cope, 1868

Bothremydidae Baur, 1891

Bothremydini Gaffney et al., 2006

Zolhafah Lapparent de Broin and Werner, 1998

Zolhafah bella Lapparent de Broin and Werner, 1998

(Figures 1–4)

Type specimen: TUB Vb-173 (MB.R. 2097), a nearly complete skull lacking the right and left cheek bones.

Type locality and horizon: Dakla Formation, Ammonite Hill member, Maastrichtian (Barthel and Herrmann-Degen, 1981; Lapparent de Broin and Werner, 1998). Ammonite Hill, south Western Desert, Egypt.

3.2 Neuroanatomical description

All internal cranial cavities of TUB Vb-173 (i.e., the endocranial, nasal, and both right and left endosseous labyrinths) are well-preserved and they have been reconstructed. The carotid and most of the nerve canals were preserved, but some of them could not be reconstructed due to the partial inner preservation of the skull of *Zolhafah bella*. The circulatory canals contained in the maxillae and premaxillae were also identified and reconstructed.

3.2.1 Endocranial cavity

The endocranial cavity of *Zolhafah bella* shows a sigmoidal shape, showing an angle between the forebrain and the hindbrain of 139° (Figures 4G, H). The dorsal surface of the anterior region of the cavity is slightly convex and reaches the cartilaginous rider at the level of the cerebral hemispheres. The dorsal surface of the hindbrain descends in a straight trajectory to reach the foramen magnum posteriorly. The olfactory bulbs region is continuous with the olfactory duct, but the limits with it and the posterior cerebral hemispheres are not clear due to the absence of boundary between them (Figure 4E). The cerebral hemispheres display the maximum width of the endocranial cavity, the ratio between the width and the length of the cavity being 0.38 (see Table 1). The cartilaginous rider is located in the posteromedial region of the cerebral hemispheres (Figures 4E, G, H). The rider is relatively long and high, representing more than 16% of the endocranial cavity length and 14% of its height (Table 1). The pituitary gland was located in the ventromedial region of the endocranial cavity, posterior to the level of the cerebral hemispheres (Figures 4F–H).

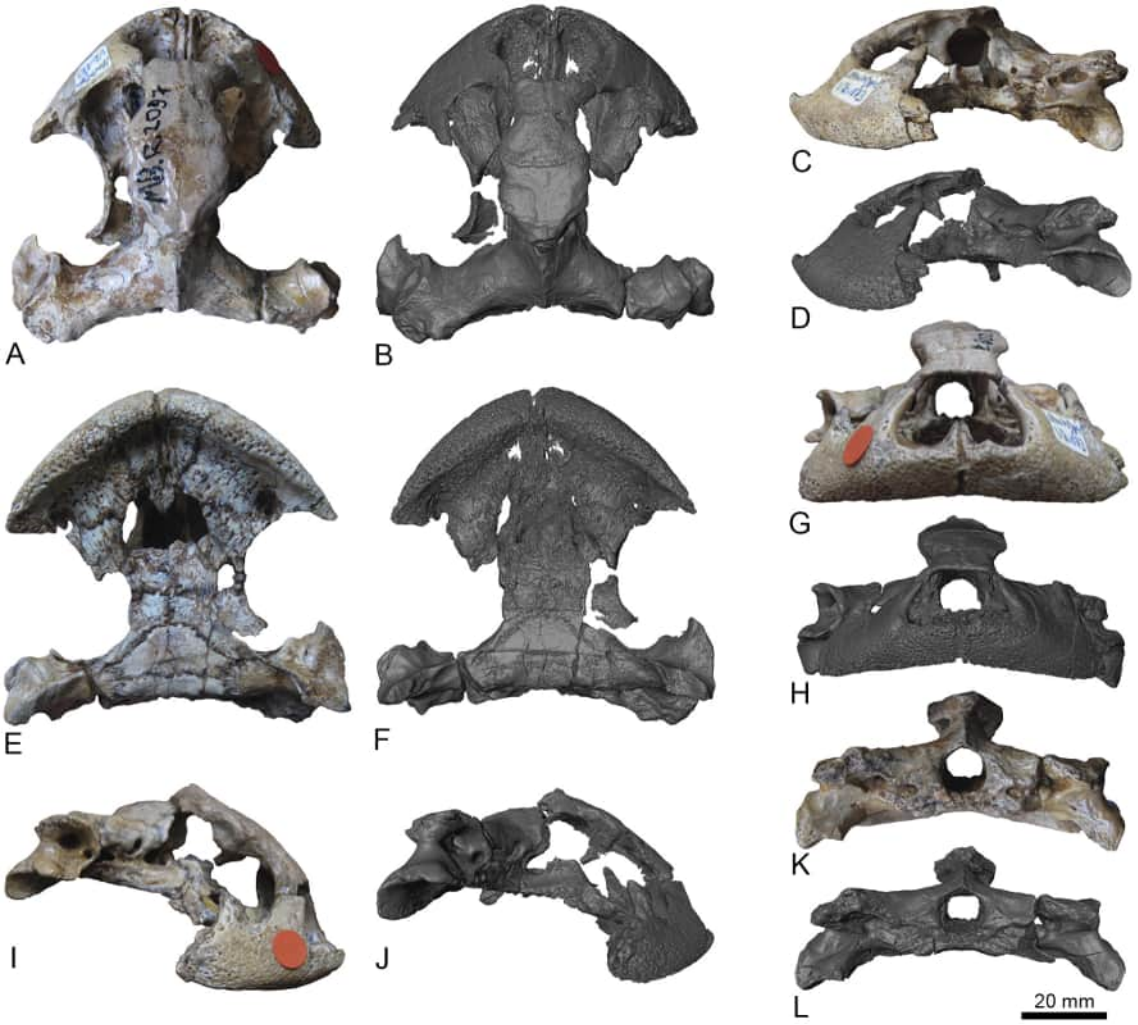

FIGURE 1
Photographs **(A, C, E, G, I, K)** and three-dimensional osseous reconstructions **(B, D, F, H, J, L)** of the skull corresponding to the holotype of *Zolhafah bella* (Pleurodira, Bothremydidae), TUB Vb-173, from the Maastrichtian of Egypt, in dorsal **(A, B)**, left lateral **(C, D)**, ventral **(E, F)**, anterior **(G, H)**, right lateral **(I, J)**, and posterior **(K, L)** views.

The pituitary fossa is a cavity excavated in the basisphenoid, laterally bordered by low clinoid processes and posteriorly by the dorsum sellae (Figures 2F, G). This fossa is oval-shaped, its major axis being anteroposteriorly directed (Figures 2F, 4F). The hindbrain corresponds to the posterior region of the endocranial cavity, being delimited by the cartilaginous rider anteriorly and the foramen magnum posteriorly (Figures 4E–H). The hindbrain displays a tubular shape, the anterior region being higher than the posterior (Figures 4G, H). The width of the medulla oblongata represents almost half of the cerebral hemispheres width (Table 1; Figure 4E).

3.2.2 Cranial nerves

The olfactory nerve (i.e., the cranial nerve I) was located in the anterodorsal region of the endocranial cavity (Figures 4A, B, E–H). The nerve ran through the olfactory sulcus, which is located at the ventromedial surface of the frontals (Figure 2D). This sulcus is relatively long and wide, representing one third of the endocranial cavity length and almost 65% of the cerebral hemispheres width (see Table 1; Figure 4E). The olfactory duct is posterodorsally directed from the nasal cavity to the olfactory bulbs region (Figures 4E, G, H). The trigeminal nerve (cranial nerve V) exited from the endocranial cavity through the foramen nervi trigemini, located in the ventrolateral surface of the endocranial cavity, posterior to the cerebral hemispheres (Figures 4G, H). The foramen is formed by the prootic posteriorly, the pterygoid ventrally, and, probably, the parietal anterodorsally, although this region is not preserved in the specimen (Figures 3D, F). This foramen is almost rounded and is the largest one of the nerve foramina (Figures 3F, 4G, H). The abducens nerve (cranial nerve VI) pierced the basisphenoid through a short and anteroposteriorly directed canal (Figure 4F). The anterior foramen of this nerve is located in the lateral surface of the clinoid process of the basisphenoid (Figure 2G), being convergent with the sulcus cavernosus. The foramen of the left abducens nerve is visible, but the canal could not be reconstructed due to the poor CT contrast between the bone and the sediment filling the posterior region of the canal. Posteriorly, the right canal reaches the dorsal surface of the basisphenoid. The facial (cranial nerve VII) and vestibulocochlear (cranial nerve VIII) nerves exited the endocranial cavity through two

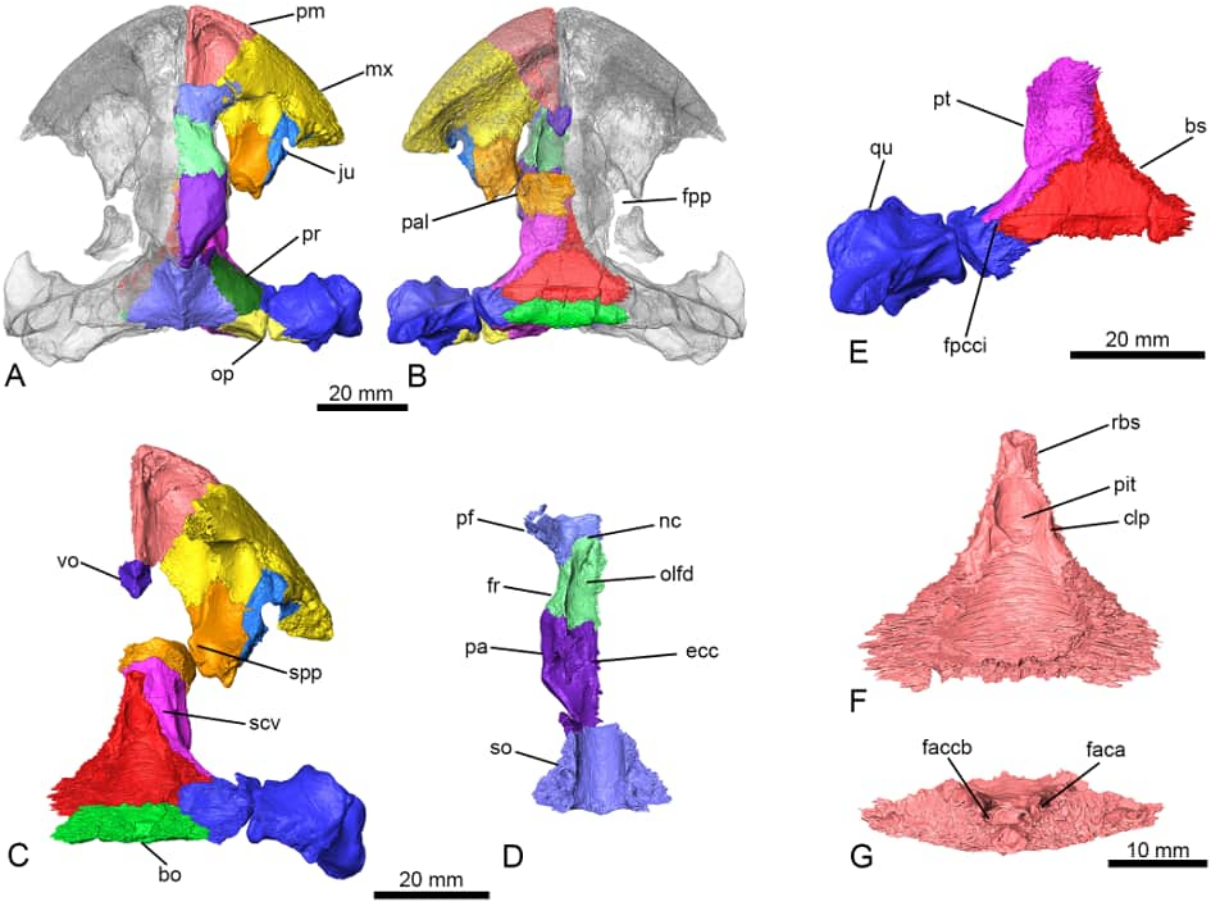

FIGURE 2
(A–D) three-dimensional osseous reconstructions of the skull corresponding to the holotype of *Zolhafah bella* (Pleurodira, Bothremydidae), TUB Vb-173, from the Maastrichtian of Egypt, in dorsal **(A, C)** and ventral **(B, D)** views. Each of the right bones was independently reconstructed. The roof bones were virtually removed in **(C)** to show the dorsal surface of the palate. The roof bones (i.e., the supraoccipital, and the right parietal, frontal, and prefrontal) are shown in ventral view in **(D)**, virtually removing the rest of the skull bones. **(E)** detail of the basisphenoid, right pterygoid, and right quadrate in ventral view. **(F, G)** detail of the basisphenoid in dorsal **(F)** and anterior **(G)** views.

foramina located in the fossa acustico-facialis (Figure 3H). The fossa is located in the medial surface of the prootic, posterior to the foramen nervi trigemini (Figures 4G, H). The canal of the facial nerve reaches the geniculate ganglion within the prootic and splits into two canals. The ventral canalis pro ramo nervi vidiani contained the vidian branch of the facial nerve (Figure 4G). The canal contacts the carotid canal. The vidian canal is not visible piercing the pterygoid due to the insufficient contrast of the images. The lateral canal that contained the hyomandibular branch of the facial nerve contacts the canalis cavernosus and exits from it posterolaterally (Figures 4E–H). The hyomandibular nerve exited the skull through the foramen chorda tympani inferius in the posteromedial region of the mandibular condyle of the quadrate (Figure 3E). The glossopharyngeal nerve (cranial nerve IX) could not be reconstructed due the poor preservation of the posterior portion of the otic region. The vagus (cranial nerve X) and spinal accessory (cranial nerve XI) nerves exited the endocranial cavity through the foramen jugulare anterior (Figures 4G, H), and they left the skull through the foramen jugulare posterius (Figure 3E). This foramen is formed by the exoccipital ventromedially and the opisthotic dorsally. Only one anterior canal of the hypoglossal nerve (cranial nerve XII) could be reconstructed due to the erosion of the posterior region of the exoccipital (Figures 4E–H). The anterior branch of the reconstructed nerve pierced the bone and exited by a ventrolateral foramen (Figure 3E).

3.2.3 Nasal cavity

The nasal opening of *Zolhafah bella* is formed by the premaxilla ventrally, the prefrontal dorsally, and the maxilla laterally (Figures 2A, C, D, 3A, C). The ventral surface of the opening is wider than the dorsal one (Figures 3A, 4C). This opening occupies a great part of the anterior region of the skull, being relatively wide (the lateral borders of the opening exceed the medial edge of the orbits; see Table 1; Figures 3A, 4C). The nasal cavity is a long and wide structure, representing 39% of the endocranial length and being almost one third wider than the cerebral hemispheres (Figures 4A, E). The volume of the nasal cavity corresponds to 43.5% of the endocast total volume, including both the endocranial and nasal cavities (see Table 1; Figures 4A–C, E-H). The antero-ventral region of the nasal cavity exhibits deep lateral depressions corresponding to the anterior portion of the nasopharyngeal ducts (Figures 4F–H). The nasopharyngeal ducts are posteriorly directed in a straight trajectory (Figure 4F). They are relatively wide and short (Figures 4F, H).

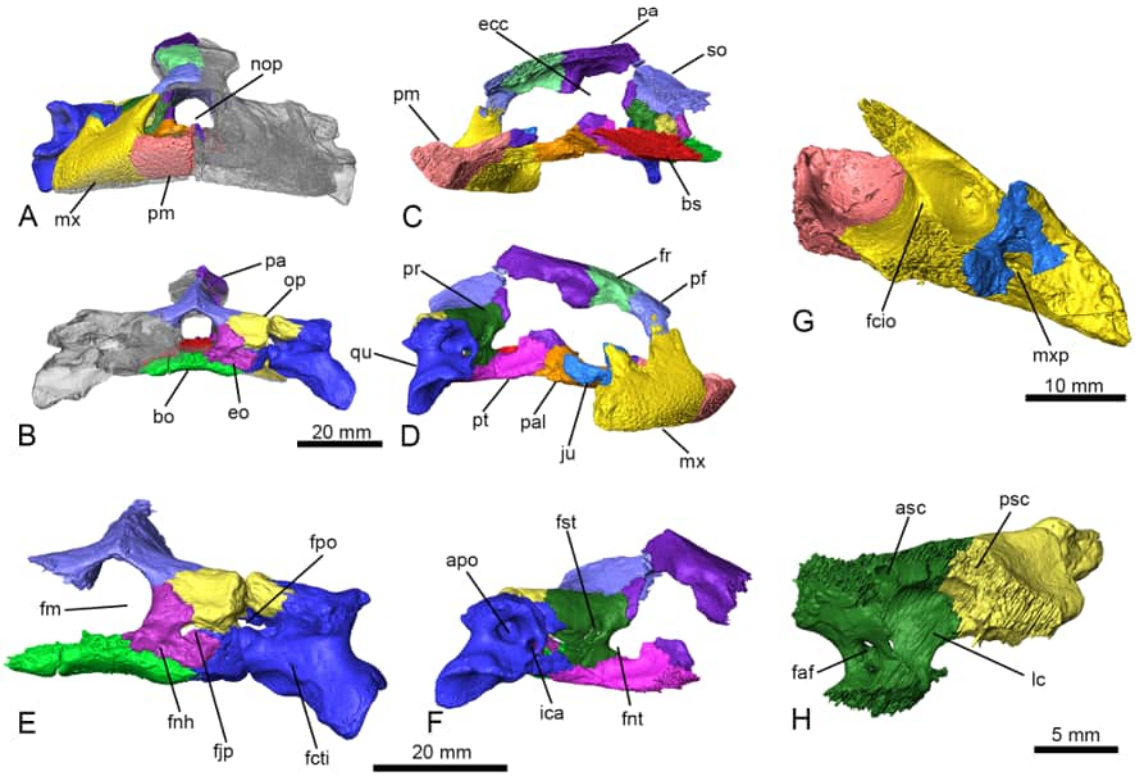

FIGURE 3
(A–D) three-dimensional osseous reconstructions of the skull corresponding to the holotype of *Zolhafah bella* (Pleurodira, Bothremydidae), TUB Vb-173, from the Maastrichtian of Egypt, in anterior **(A)**, posterior **(B)**, left lateral **(C)**, and right lateral **(D)** views. **(E)** posterior region of the skull, in posterior view, virtually removing the left side. **(F)** right lateral region of the skull, in lateral view, virtually removing the anterior portion of the skull. **(G)** right premaxilla, maxilla, and jugal, in posterior view. **(H)** right prootic and opisthotic, in medial view.

3.2.4 Endosseous labyrinth

The endosseous labyrinth shows low and relatively narrow semicircular canals (Figures 4I–L). The anterior canal of both right and left labyrinths is formed by the prootic and the supraoccipital (Figure 3H), being the longest canal (see Table 1; Figures 4I–L). The posterior canal is formed by the supraoccipital and the opisthotic (Figure 3H). The lateral canal is formed by the prootic and the opisthotic, being the widest canal of the endosseous labyrinth (Figures 4I–L). The dorsal surfaces of the anterior and the posterior semicircular canals are at the same level (Figures 4I, K), with the apex of the crus communis located below them. The crus communis is slightly longer than high. The values of the ratio between the height and the length of the endosseous labyrinth are 1.45 and 1.46, considering the left and right labyrinths respectively. The angle formed by the dorsal semicircular canals (i.e., the anterior and posterior ones) is acute, its value being about 78° in both labyrinths (Figures 4J, L). The space formed between the semicircular canals and the dorsal surface of the vestibulum is elongated anteroposteriorly and narrow dorsoventrally (Figures 4I, K).

3.2.5 Cranial circulatory system

The cranial circulatory system is composed of a series of canals that contained the arteries and veins. The internal carotid entered the skull posteriorly and bifurcated outside the cranial bones. The medial branch corresponds to the cerebral branch of the carotid artery and the dorsal one corresponds to the stapedial artery. The carotid artery entered the skull through the foramen posterius canalis carotici interni, formed by the basisphenoid, pterygoid, and quadrate (Figures 2E, 4B). The canal is anteromedially directed to contact the pituitary fossa posteriorly through the foramen anterius canalis carotici basisphenoidalis (Figures 2G, 4B, F). The angle formed by the carotid canals shows a value of almost 96° (Figures 4B, F). The stapedial artery ran through the canalis stapedio-temporalis which is anterodorsally directed (Figure 4E). The foramen stapedio-temporalis is formed by the prootic and is anteriorly directed (Figure 3F). The stapedial artery entered the fossa temporalis through this foramen and reached the posterior end of the medial process of the maxilla through the foramen canalis infraorbitalis (Figures 3G, 4E, G). The portion of the artery that entered the maxilla corresponds to the infraorbital artery. This artery bifurcated and continued as the inframaxillary artery, piercing the maxilla posterolaterally through the posterior portion of the infraorbital canal. The anterior section of the artery contacts the canalis alveolaris superior, which contained the supramaxillary artery. This artery bifurcates again, the medial branch forming the posterior nasal artery that supplies part of the nasal cavity (Figure 4G). The anterior arterial canals show numerous branches (Figures 4A–C, E, G), contacting the external surface of the maxilla and premaxilla through the foramina (Figures 3A, D).

The lateral cerebral vein ran posteriorly crossing the sulcus cavernosus and continued through the canalis cavernosus (Figure 4F). This vein exited from the skull through the fenestra postotica (Figures 3E, 4D) sharing the opening with the stapedial artery. The fenestra postotica is formed by the opisthotic dorsally

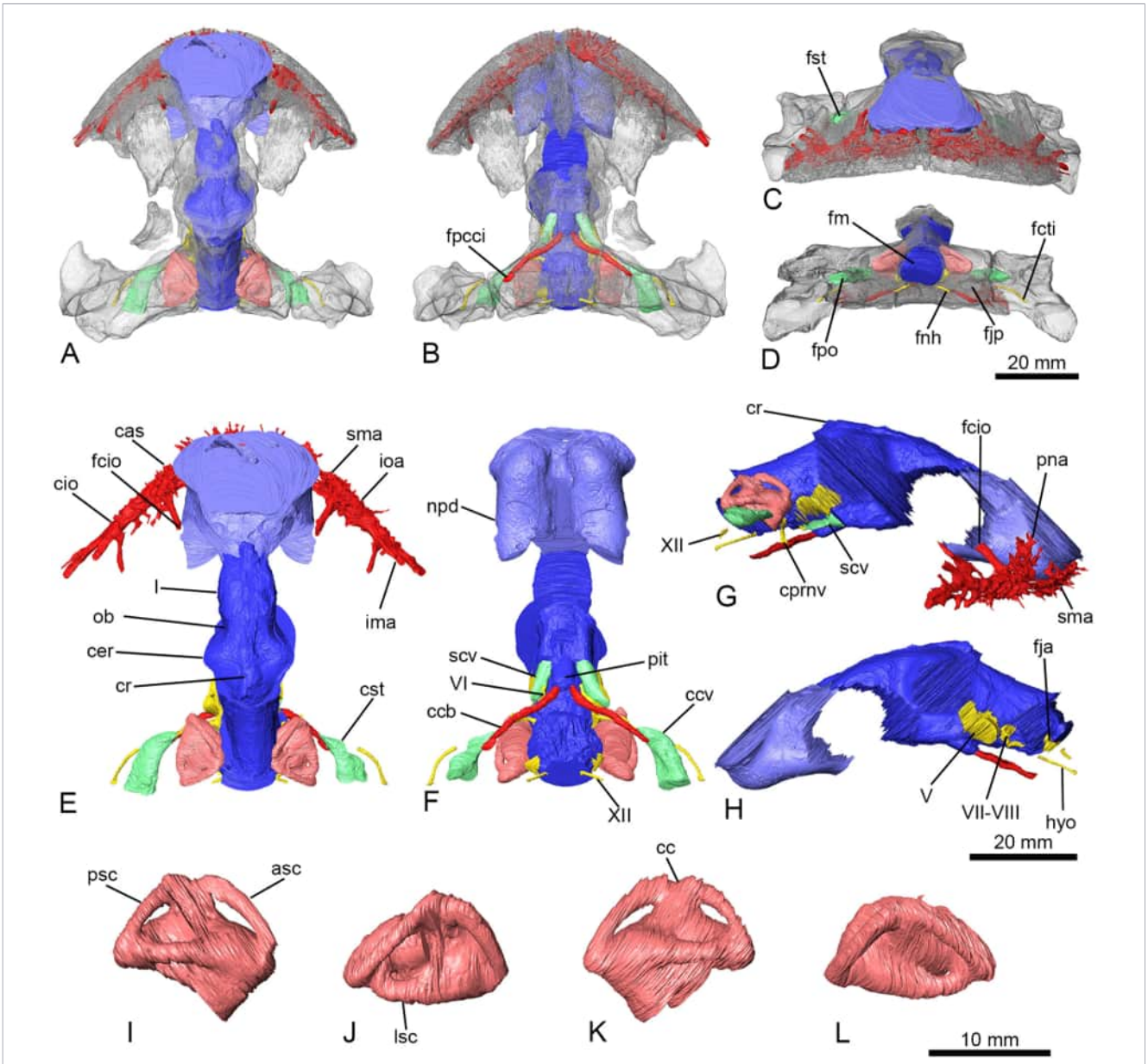

FIGURE 4
Neuroanatomical virtual three-dimensional reconstructions of the skull corresponding to the holotype of *Zolhafah bella* (Pleurodira, Bothremydidae), TUB Vb-173, from the Maastrichtian of Egypt. **(A–D)** complete neuroanatomical reconstructions with the fossil transparented, in dorsal **(A)**, ventral **(B)**, anterior **(C)**, and posterior **(D)** views. **(E-H)** complete neuroanatomical reconstructions virtually removing the skull, in dorsal **(E)**, ventral **(F)**, right lateral **(G)**, and left lateral **(H)** views. The maxillary vascular canals were virtually removed in **(F, H)** to show the nasal cavity, and the canalis cavernosus and the left endosseous labyrinth were virtually removed in **(H)** to show the left nerves. **(I, J)** right endosseous labyrinth, in lateral **(I)** and dorsal **(J)** views. **(K, L)** left endosseous labyrinth, in lateral **(K)** and dorsal **(L)** views.

and the quadrate ventrally (Figure 3E). The other main venous vessel corresponds to the posterior cerebral vein (i.e., the jugular vein). This vein left the skull through the foramen jugulare posterius (Figures 3E, 4D), sharing the opening with the nerves.

4 Discussion

The three-dimensional virtual osseous and neuroanatomical reconstructions of the skull corresponding to the holotype of *Zolhafah bella*, TUB Vb-173, are generated in the present work. Although previous descriptions of the skull of *Zolhafah bella* provide detailed information (see Lapparent de Broin and Werner, 1998; Gaffney et al., 2006), the new three-dimensional models of the cranial bones allow us to re-evaluate some previous interpretations. The detailed analysis of both jugals allows us to propose that the putative posterior opening of the maxillary pits described by Gaffney et al. (2006) cannot be recognized as characteristic of this taxon, but rather as an artifact generated by the poor preservation of this region (Figures 1A, B, E, F, 2A–C, 3G). Contrary to the description of Lapparent de Broin and Werner (1998), the new detailed analysis of the anterior palatal region from the three-dimensional models shows that the contact between the

TABLE 1 Measurements of the neuroanatomical elements of the holotype of *Zolhafah bella* (Pleurodira, Bothremydidae), TUB Vb-173, from the Maastrichtian of Egypt.

Neuroanatomical element		Measurement	Value
Endocranial cavity		Total length	45.8
		Cerebral hemispheres width	17.5
		Medulla oblongata width	9.2
		Cartilaginous rider length	7.4
		Cartilaginous rider height	2.7
		Olfactory nerve length	15.3
		Olfactory nerve width	11.3
Nasal cavity		Nasal opening height	11.6
		Nasal opening width	18.7
		Nasal cavity length	18.7
		Nasal cavity width	23.2
		Relative volume	43.5%
Endosseous labyrinth	Rigth	Length	12.6
		Height	7.5
		Angle canals	78.1°
		ASC length	5.6
		PSC length	5.2
		LSC length	4.6
	Left	Length	13.3
		Height	7.8
		Angle canals	77.5°
		ASC length	5.9
		PSC length	5.5
		LSC length	3.8

Linear measurements in mm, and angular measurements in degrees. The volume of the nasal cavity represents the percentage occupied by the cavity relative to the complete endocast. The length considered for the endocranial cavity includes that of the olfactory duct.

vomer and the maxilla is absent in the specimen (Figures 2B, C), confirming the observations of Gaffney et al. (2006).

Regarding neuroanatomical aspects, the three-dimensional reconstruction of the endocranial cavity of *Zolhafah bella* were compared with those of several taxa of bothremydids represented by only one specimen, so it was not possible to evaluate intraspecific differences within each species. This could represent a limitation when interpreting interspecific differences at the ecological and/or functional level. The endocranial cavity of *Zolhafah bella* allows us to observe a combination of neuroanatomical characters exclusive to Bothremydidae within Pleurodira (Martín-Jiménez and Pérez-García, 2021). The cavity shows a value of the angle formed by the forebrain and the hindbrain less than 150° (i.e., 139° for the only known specimen of the species, see Figures 4G, H), as occurs in all other representatives of Bothremydidae in which this feature had been measured (the angle values range between approximately 133° for *Bothremys cooki* and *Azzabaremys moragjonesi*, and 149° for *Galianemys emringeri*; see Table 2; Martín-Jiménez and Pérez-García, 2022, 2025a). This feature is also shared with the sister group Podocnemidoidae (Ferreira et al., 2018; Hermanson et al., 2020; Martín-Jiménez and Pérez-García, 2021, 2025b), the value of this angle being greater than 150° in other lineages of Pleurodira (i.e., Chelidae, Pelomedusidae, Araripemydidae, and Euraxemydidae; Hermanson et al., 2020; Martín-Jiménez and Pérez-García, 2021, 2023). The presence of a relatively long and high cartilaginous rider in the dorsal surface of the cavity is shared with all members of Bothremydidae known so far (Gaffney and Zangerl, 1968; Martín-Jiménez and Pérez-García, 2021, 2022, 2025a, b). Most representatives of Podocnemidoidae lack this structure or show a reduced rider, being posterodorsally expanded in some members of Podocnemididae (Ferreira et al., 2018; Hermanson et al., 2020; Werneburg et al., 2021; Martín-Jiménez and Pérez-García, 2021, 2025c). The other character exclusively shared by most Podocnemidoidea (i.e., Bothremydidae and the sister group Podocnemidoidae), with the exception of Nigeremydini within Pleurodira is the presence of a geniculate ganglion located in the prootic in which the facial nerve splits and the vidian branch pierces the bone anteroventrally through a canalis pro ramo nervi vidiani (Rollot et al., 2021; Martín-Jiménez and Pérez-García, 2021, 2022, 2023, 2025c). This pattern, also observed for *Zolhafah bella*, differs in the bothremydid lineage of Nigeremydini in which the geniculate ganglion is located in the canalis cavernosus (Martín-Jiménez and Pérez-García, 2025a).

The relatively wide olfactory sulcus in *Zolhafah bella* is similar to that in the representatives of Taphrosphyini *Phosphatochelys tedfordi* and *Taphrosphys ippolitoi* (Martín-Jiménez and Pérez-García, 2025b). Contrary to the condition observed for these taxa, the olfactory nerve of Cearachelyini, Nigeremydini, and all other members of Bothremydini is narrower (Martín-Jiménez and Pérez-García, 2021, 2022, 2025a). In addition, the relative length of this nerve measured for *Zolhafah bella* is greater than that in all other Bothremydini which are identified as freshwater forms (i.e., being equivalent to one third of the total length of the endocast for *Zolhafah bella* but approximately 20% of the cavity in *Tartaruscola teodorii* and *Chedighaii* sp., and almost 30% in *Bothremys cooki* and *Chedighaii barberi*; see Table 2; Martín-Jiménez and Pérez-García, 2021, 2022). The presence of a long olfactory sulcus is also observed in the pelagic bothremydid *Azzabaremys moragjonesi*, being equivalent to 44% of the endocast length (Martín-Jiménez and Pérez-García, 2025a). However, the value ranges between less than 20% and almost 30% for the representatives of the coastal lineage of Taphrosphyini in which this character is known (i.e., *Taphrosphys ippolitoi* and *Phosphatochelys tedfordi* respectively; Hermanson et al., 2020; Martín-Jiménez and Pérez-García, 2025b). The overlap of nerve length values between coastal and freshwater forms does not allow us to suggest a direct relationship between the length of the structure and the lifestyle of each species. Although larger sample size in future studies will allow for a better ecological interpretation of this feature, in this case the relative length of the olfactory sulcus could represent and additional evidence, along with the relative width, regarding the lifestyle of different representatives of Bothremydidae.

TABLE 2 Comparative measurements, values, and ratios of some neuroanatomical elements of the representatives of Bothremydidae (Testudines, Pleurodira) in which these were documented.

Clade	Species	Specimen number	Reference	ECA	OL/TL	L L/H	NCV	CCA
Cearachelyini	*Galianemys whitei*	MNHN MRS 2098	Martín-Jiménez and Pérez-García (2022)	148	14.9	2.28	22.6	79
	Galianemys emringeri	MNHN MRS 3105		149	14.4	2.81	28.6	71
Bothremydini	*Zolhafah bella*	TUB Vb-173	This study	139	33.3	1.46	43.5	96
	Tartaruscola teodorii	MNHN.F.SPP33	Martín-Jiménez and Pérez-García (2021)	–	–	3.06	–	98
		MNHN.F.SPP34		145	21.6	–	22.8	109
	Bothremys cooki	AMNH 2521	Gaffney and Zangerl (1968)	–	27.9	–	–	–
	Chedighaii barberi	FMNH PR 247	Gaffney and Zangerl (1968)	133	29.0	–	–	–
	Chedighaii sp.	YPM PU 12951	Gaffney (1977)	–	19.5	–	–	–
	Bothremys maghrebiana	AMNH 30324	Hermanson et al. (2020)	–	–	2.91	–	–
Taphrosphyini	*Taphrosphys ippolitoi*	GBE-450	Martín-Jiménez and Pérez-García (2025b)	147	19.7	1.79	–	116
	Phosphatochelys tedfordi	AMNH 30008	Hermanson et al. (2020)	120	28.7	–	–	
	Ummulisani rutgersensis	AMNH 30569	Hermanson et al. (2020); Evers et al. (2022)	–	–	1.93	–	>140
Nigeremydini	*Azzabaremys moragjonesi*	NHMUK R16370	Martín-Jiménez and Pérez-García (2025a)	134	44.0	1.98*	54.2	89

ECA, endocranial cavity angle; OL/TL, ratio between the length of the olfactory duct and that of the total endocranial cavity length; L L/H, ratio between the length and the height of the endosseous labyrinth; NCV, nasal cavity volume; CCA, carotid canals angle. Angular measurements in degrees. The volume of the nasal cavity represents the percentage occupied by the cavity relative to the complete endocast.

The enlarged nasal opening and the nasal cavity observed for *Zolhafah bella* are also present in the marine coastal and open sea bothremydids, Taphrosphyini and Nigeremydini respectively (Gaffney et al., 2006; Pérez-García, 2019). The high relative volume of the nasal cavities of *Zolhafah bella* is lower than that observed in the Nigeremydini *Azzabaremys moragjonesi* [representing 43% of the endocast volume in the first taxon and more than half in the latter (Martín-Jiménez and Pérez-García, 2025a)]. The size of the nasal opening in *Zolhafah bella* and *Azzabaremys moragjonesi* is directly related to the volume of the nasal cavity. However, the volume of the nasal cavities of the representatives of Taphrosphyini has not been measured so far, so it cannot be verified whether they also share this condition. The nasal opening observed for the freshwater forms of Bothremydidae is not enlarged, in contrast with the condition in marine lineages (Martín-Jiménez and Pérez-García, 2021, 2022). Thus, the nasal cavities of the Cearachelyini and the freshwater Bothremydini are smaller than marine forms, with the relative volume being approximately 20% of the endocast volume (including the nasal and endocranial cavities; see Table 2). Enlarged nasal cavities have also been observed in different lineages of terrestrial turtles, both representatives of the stem group and testudinid cryptodires (Lautenschlager et al., 2018; Paulina-Carabajal et al., 2017). In these tortoises, it has been suggested that the large size of the nasal cavities (in convergence with those in the marine bothremydids) could reflect an adaptive response to terrestrial environments, related to other capabilities such as thermoregulation or communication (Lautenschlager et al., 2018; Paulina-Carabajal et al., 2017).

The endosseous labyrinth of *Zolhafah bella* presents relatively short and high semicircular canals compared to those of freshwater bothremydids (Hermanson et al., 2020; Martín-Jiménez and Pérez-García, 2021, 2022). Thus, the ratio between the length and the height of the labyrinth of *Zolhafah bella* is lower than 1.50, whereas this ratio ranges between 2.26 and 3.06 in Cearachelyini and freshwater Bothremydini, showing more elongated and low semicircular canals (see Table 2). As observed in *Zolhafah bella*, the labyrinth of marine bothremydids shows values close to or less than 2.0, having been identified as 1.91 and 2.05 respectively for the right and left inner ears of the holotype of the Nigeremydini *Azzabaremys moragjonesi*, and as 1.79 for the Taphrosphyini representatives *Taphrosphys ippolitoi* and 1.93 for *Ummulisani rutgersensis* (Evers et al., 2022; Martín-Jiménez and Pérez-García, 2025a, b). Although recent studies do not show a direct relationship between lifestyle of the turtles and the endosseous labyrinth morphology (Evers et al., 2022), the relative proportions between the length and the height of the semicircular canals allow the identification of freshwater forms with elongated and low canals, and marine forms with short and high canals within Pleurodira (Martín-Jiménez and Pérez-García, 2021, 2022, 2023, 2025a, –, c).

The carotid arteries of Bothremydidae enter the skull posteriorly from the foramina canalis carotici interni. This condition contrasts with that in the representatives of its sister group Podocnemidoidae, in which the carotid vessels enter through the cavum pterygoidei (Gaffney et al., 2006, 2011; Rollot et al., 2021). The angle formed by the carotid canals in *Zolhafah bella* is obtuse, with a value lower than that in the other Bothremydini in which this measurement is known (i.e., *Tartaruscola teodorii*; see Table 2; Martín-Jiménez and Pérez-García, 2021). The value of that angle is intermediate between those most acute in

Cearachelyini and more obtuse in Taphrosphyini (Hermanson et al., 2020; Martín-Jiménez and Pérez-García, 2022, 2025b). Despite most pleurodires having lost the supramaxillary foramen, the extant genus *Podocnemis*, the Brazilian Albian euraxemydid *Euraxemys essweini* Gaffney et al., 2006, and some bothremydids (including the Bothremydini *Bothremys cooki* and *Zolhafah bella*, and the Moroccan Paleogene Taphrosphyini *Rhothonemys brinkmani* Gaffney et al., 2006), retain a foramen for the maxillary artery (Tada et al., 2025, and references therein). The three-dimensional reconstruction of the vascular maxillary canals of *Zolhafah bella* performed in the present work allows the confirmation of the presence of this foramen and the splitted arterial canal (Figures 4E, G). In addition, this pattern has also recently been observed for the Nigeremydini *Azzabaremys moragjonesi* and the Taphrosphyini *Taphrosphys ippolitoi*, displaying bifurcated maxillary arteries (Martín-Jiménez and Pérez-García, 2025a, b). However, the maxillary canals of *Zolhafah bella* differ from those of the other bothremydids in which the maxillar canals were reconstructed, being wider (Martín-Jiménez and Pérez-García, 2025a, b). Unlike the canals of other bothremydids, those of *Zolhafah bella* have numerous ramifications (Figures 4A–C, E, G). However, the arteries that did not run through bony canals could not be reconstructed for *Zolhafah bella*, so the complete cranial vascular system is unknown for this taxon. In the case of the extant cryptodires, the anterior vessels were analyzed from dissections and three-dimensional reconstructions generated from CT scan (e.g., Albrecht, 1976; Tada et al., 2025). Despite the cranial arterial system of extant sea turtles is related to the vascularization of the salt glands, the maxillary artery does not participate in this role (Yoshida et al., 2022). Thus, the function of the maxillary vascularization of *Zolhafah bella* is not clear. The irrigation of the maxillary and nasal region of this bothremydid taxon could be result from adaptations to a marine environment. However, for a proper evaluation of the morphology and branching of the maxillary canals, a more detailed study of the vascular system in marine and potentially marine turtle forms (both extant and extinct cryptodires and pleurodires) would be necessary, expanding the comparative sample in order to test this hypothesis.

5 Conclusions

This work represents the first three-dimensional osseous reconstruction and the first neuroanatomical study of the Bothremydini species *Zolhafah bella* (Pleurodira, Bothremydidae), from the Maastrichtian of Egypt. This study is based on the holotype and only documented specimen attributable to the species.

Neuroanatomical analysis provides greater robustness to the neuroanatomical characterization of the Bothremydidae lineage, which was poorly understood until recent years. Some of the features recognized as exclusively shared by all of them include, among others, an angle between the forebrain and the hindbrain lesser than 150°, which gives the endocranial cavity a sigmoidal morphology, and the presence of a prominent dorsal cartilaginous rider.

The representatives of the lineage Cearachelyini are completely identified as freshwater forms. Other lineages of Bothremydidae have been recognized as littoral (i.e., Taphrosphyini) or even marine pelagic (i.e., Nigeremydini). *Zolhafah bella* is a member of Bothremydini, a lineage that appears to exhibit a broad versatility, with representatives adapted to both continental and, probably, littoral environments. However, the interpretation of some members of this lineage as marine was based exclusively on indirect data, especially sedimentological interpretations of the outcrops where they were found. The neuroanatomical study of *Zolhafah bella* conducted here shows that, contrary to the other Bothremydini representatives (e.g., *Tartaruscola teodorii* or *Bothremys cooki*), it was a turtle adapted to marine environments. Comparison with other members of the lineage, in which different neuroanatomical elements have been analyzed, has allowed the identification of convergent characters with marine bothremydid of coastal and open sea lineages. Thus, the relatively enlarged nasal cavity of *Zolhafah bella* and the relatively short and high semicircular canals allow to characterize this taxon as a marine form. The presence of very wide and ramificated vascular canals in maxilla of the specimen here analyzed is a feature recognized as exclusive within Bothremydidae, and may also be related to adaptations to a marine environment. The results obtained expand our knowledge about the bothremydid species *Zolhafah bella*, and modify our understanding of the comparative neuroanatomical framework within Bothremydidae.

Data availability statement

Publicly available datasets were analyzed in this study. The specimen of Zolhafah bella (TUB Vb-173) is housed in the palaeontological collection of the Museum für Naturkunde (Berlin, Germany). The obtained three-dimensional models of the bones and the neuroanatomical structures of Zolhafah bella are available in MorphoSource, https://www.morphosource.org/projects/000860595 (accessed May 16, 2026).

Author contributions

MM: Conceptualization, Data curation, Formal analysis, Investigation, Methodology, Software, Validation, Visualization, Writing – original draft, Writing – review & editing. AP-G: Conceptualization, Funding acquisition, Investigation, Project administration, Resources, Supervision, Validation, Writing – original draft, Writing – review & editing.

Funding

The authors declared that financial support was received for this work and/or its publication. This research work is funded by the Ministerio de Ciencia e Innovación (research project PID2023-148083NB-I00).

Acknowledgments

The authors thank the Museum für Naturkunde staff, especially Daniela Schwarz, for access to the specimen analyzed here, as well as for the permission and arrangements to scan it. This research was funded by the Spanish Ministerio de Ciencia, Innovación y Universidades (research project PID2023-148083NB-I00).

Conflict of interest

The authors declared that this work was conducted in the absence of any commercial or financial relationships that could be construed as a potential conflict of interest.

The authors AP-G declared that they were an editorial board member of Frontiers, at the time of submission. This had no impact on the peer review process and the final decision.

Generative AI statement

The authors declared that generative AI was not used in the creation of this manuscript.

Any alternative text (alt text) provided alongside figures in this article has been generated by Frontiers with the support of artificial intelligence and reasonable efforts have been made to ensure accuracy, including review by the authors wherever possible. If you identify any issues, please contact us.

Publisher's note

References

Albrecht, P. W. (1976). The cranial arteries of turtles and their evolutionary significance. *J. Morphol.* 149, 159–182. doi: 10.1002/jmor.1051490203

Barthel, K. W., and Herrmann-Degen, W. (1981). Late cretaceous and early tertiary stratigraphy in the Great Sand Sea and its SE margins (Farafra and Dakhla Oases), SW Desert, Egypt. *Mitt. Bayer. Staatsslg. Paläont. Hist. Geol.* 21, 141–182.

Batsch, G. C. (1788). *Versuch Einer Anleitung, Zur Kenntniß Und Geschichte Der Thiere Und Mineralien* (Jena: Akademie Buchhandlung), 528 pp.

Baur, G. (1891). Notes on some little known American fossil tortoises. *Proc. Acad. Nat. Sci. Phil.* 43, 411–430.

Cadena, E. A., Bloch, J. I., and Jaramillo, C. A. (2012). New bothremydid turtle (Testudines, Pleurodira) from the Paleocene of Northeastern Colombia. *J. Paleont.* 86, 688–698. doi: 10.1666/11-128R1.1

Cope, E. D. (1864). On the limits and relations of the Raniformes. *Proc. Acad. Nat. Sci. Phil.* 16, 181–183.

Cope, E. D. (1868). On the origin of genera. *Proc. Acad. Nat. Sci. Phil.* 20, 242–300.

Evers, S. W., Joyce, W. G., Choiniere, J. N., Ferreira, G. S., Foth, C., Hermanson, G., et al. (2022). Independent origin of large labyrinth size in turtles. *Nat. Commun.* 13, 5807. doi: 10.1038/s41467-022-33091-5

Ferreira, G. S., Iori, F. V., Hermanson, G., and Langer, M. C. (2018). New turtle remains from the Late Cretaceous of Monte Alto-SP, Brazil, including cranial osteology, neuroanatomy and phylogenetic position of a new taxon. *Paläontol. Z.* 92, 481–498. doi: 10.1007/s12542-017-0397-x

Ferreira, G. S., Werneburg, I., Lautenschlager, S., and Evers, S. W. (2023). "Contrasting brains and bones: Neuroanatomical evolution of turtles (Testudinata)," in *Paleoneurology of Amniotes*. Eds. M. T. Dozo, A. Paulina-Carabajal, T. E. Macrini and S. Walsh (Switzerland: Springer), 79–121. doi: 10.1007/978-3-031-13983-3_4

Gaffney, E. S. (1977). An endocranial cast of the side-necked turtle, *Bothremys*, with a new reconstruction of the palate. *Am. Mus. Novit.* 2639, 1–12.

Gaffney, E. S., Meylan, P. A., Wood, R. G., Simons, E., and de Almeida Campos, D. (2011). Evolution of the side-necked turtles: the family Podocnemididae. *Bull. Am. Mus. Nat. Hist.* 350, 1–237. doi: 10.1206/350.1

Gaffney, E. S., Moody, R. T. J., and Walker, C. A. (2001). *Azabbaremys*, a new sidenecked turtle (Pelomedusoides: Bothremydidae) from the Paleocene of Mali. *Am. Mus. Novit.* 3320, 1–16. doi: 10.1206/0003-0082(2001)320%3C0001:AANSNT%3E2.0.CO;2

Gaffney, E. S., and Tong, H. (2003). *Phosphatochelys*, a new side-necked turtle (Pelomedusoides: Bothremydidae) from the Paleocene of Morocco. *Bull. Am. Mus. Nat. Hist.* 279, 644–659. doi: 10.1206/0003-0090(2003)279%3C0644:C%3E2.0.CO;2

Gaffney, E. S., Tong, H., and Meylan, P. E. (2002). *Galianemys*, a new side-necked turtle (Pelomedusoides: Bothremydidae) from the late cretaceous of Morocco. *Am. Mus. Novit.* 3379, 1–20. doi: 10.1206/0003-0082(2002)379%3C0001:GANSNT%

Gaffney, E. S., Tong, H., and Meylan, P. E. (2006). Evolution of the side-necked turtles: The families Bothremydidae, Euraxemydidae, and Araripemydidae. *Bull. Am. Mus. Nat. Hist.* 300, 1–698. doi: 10.1206/0003-0090(2006)300[1:eotstt]2.0.co;2

Gaffney, E. S., and Zangerl, R. (1968). A revision of the chelonian genus *Bothremys* (Pleurodira: Pelomedusidae). *Fieldiana Geol.* 16, 193–239. doi: 10.5962/bhl.title.5195

Hermanson, G., Benson, R. B. J., Farina, B. M., Ferreira, G. S., Langer, M. C., and Evers, S. W. (2022). Cranial ecomorphology of turtles and neck retraction as a possible trigger of ecological diversification. *Evolution* 76-11, 2566–2586. doi: 10.1111/evo.14629

Hermanson, G., Iori, F. V., Evers, S. W., Langer, M. C., and Ferreira, G. S. (2020). A small podocnemidoid (Pleurodira, Pelomedusoides) from the late cretaceous of Brazil, and the innervation and carotid circulation of side-necked turtles. *Pap. Palaeontol.* 6, 329–347. doi: 10.1002/spp2.1300

Hudson, D. M., and Lutz, P. L. (1986). Salt gland function in the leatherback sea turtle, *Dermochelys coriacea*. *Copeia* 1986, 247–249. doi: 10.2307/1444922

Lapparent de Broin, F. (2000). African chelonians from the Jurassic to the present: Phases of development and preliminary catalogue of the fossil record. *Palaeont. Afr.* 36, 43–82.

Lapparent de Broin, F., Metais, G., Bartolini, A., Brohi, I. A., Lashari, R. A., Marivaux, L., et al. (2021). First report of a bothremydid turtle, *Sindhochelys ragei* n. gen. n. sp. from the early Paleocene of Pakistan, systematic and palaeobiogeographic implications. *Geodiversitas* 43, 1341–1363. doi: 10.5252/geodiversitas2021v43a25

Lapparent de Broin, F., and Werner, C. (1998). New late cretaceous turtles from the Western Desert. Egypt. *Ann. Paléontol.* 84, 131–214. doi: 10.1016/S0753-3969(98)80005-0

Lautenschlager, S., Ferreira, G. S., and Werneburg, I. (2018). Sensory evolution and ecology of early turtles revealed by digital endocranial reconstructions. *Front. Ecol. Evol.* 6, 7. doi: 10.3389/fevo.2018.00007

Leidy, J. (1865). Cretaceous reptiles of the United States. *Smithsonian Contributions to knowledge* 192, 1–135. doi: 10.5962/bhl.title.39830

Maniel, I. J., de la Fuente, M. S., and Canale, J. I. (2021). The first Cearachelyini (Pelomedusoides, Bothremydidae) turtle from the Upper Cretaceous of Patagonia, and an overview of the occurrence and diversity of Pelomedusoides in Patagonia. *Cret. Res.* 125, 104869. doi: 10.1016/j.cretres.2021.104869

Marshall, A. T., and Cooper, P. D. (1988). Secretory capacity of the lacrimal salt gland of hatchling sea turtles, *Chelonia mydas*. *J. Comp. Physiol. B* 157, 821–827. doi: 10.1007/BF00691014

Martín-Jiménez, M., and Pérez-García, A. (2021). Neuroanatomical study and three-dimensional reconstruction of the skull of a bothremydid turtle (Pleurodira) based on the European Eocene *Tartaruscola teodorii*. *Diversity* 13, 298. doi: 10.3390/d13070298

Martín-Jiménez, M., and Pérez-García, A. (2022). The neuroanatomy of the bothremydid pleurodiran turtle *Galianemys*, from the Late Cretaceous (Cenomanian) of Morocco. *Anat. Rec.* 306, 1377–1395. doi: 10.1002/ar.25072

Martín-Jiménez, M., and Pérez-García, A. (2023). Neuroanatomical study and three-dimensional cranial recon-struction of the Brazilian Albian pleurodiran turtle *Euraxemys essweini*. *Diversity* 15, 374. doi: 10.3390/d15030374

Martín-Jiménez, M., and Pérez-García, A. (2025a). The first neuroanatomical study of a marine pleurodire (the large Paleocene bothremydid *Azzabaremys moragjonesi*) reveals

convergences with other clades of pelagic turtles. *Foss. Rec.* 28, 1–15. doi: 10.3897/fr.28.130418

Martín-Jiménez, M., and Pérez-García, A. (2025b). First neuroanatomical study of the Paleocene bothremydid turtle *Taphrosphys* (Pleurodira), based on a skull of the Moroccan *Taphrosphys ippolitoi*, and implications for the marine lifestyle in Taphrosphyini. *Swiss J. Palaeontol.* 144, 66. doi: 10.1186/s13358-025-00401-5

Martín-Jiménez, M., and Pérez-García, A. (2025c). Neuroanatomical study of the podocnemidid turtle *Neochelys arenarum* (Pleurodira), from the early Eocene of France. *Anat. Rec.* 308, 1646–1658. doi: 10.1002/ar.25217

Neenan, J. M., Reich, T., Evers, S. W., Druckenmiller, P. S., Voeten, D. F. A. E., Choiniere, J. N., et al. (2017). Evolution of the sauropterygian labyrinth with increasingly pelagic lifestyles. *Curr. Biol.* 27, 3852–3868. doi: 10.1016/j.cub.2017.10.069

Parsons, T. S. (1959). Nasal anatomy and the phylogeny of reptiles. *Evolution* 13, 175–187. doi: 10.1111/j.1558-5646.1959.tb03003.x

Paulina-Carabajal, A., Sterli, J., Georgi, J., Poropat, S. F., and Kear, B. P. (2017). Comparative neuroanatomy of extinct horned turtles (Meiolaniidae) and extant terrestrial turtles (Testudinidae), with comments on the palaeobiological implications of selected endocranial features. *Zool. J. Linn. Soc* 180, 930–950. doi: 10.1093/zoolinnean/zlw024

Pérez-García, A. (2016a). A new turtle confirms the presence of Bothremydidae (Pleurodira) in the Cenozoic of Europe and expands the biostratigraphic range of Foxemydina. *Sci. Nat.* 103, 14. doi: 10.1007/s00114-016-1375-y

Pérez-García, A. (2016b). A new turtle taxon (Podocnemidoidea, Bothremydidae) reveals the oldest known dispersal event of the crown Pleurodira from Gondwana to Laurasia. *J. Syst. Palaeontol.* 2016, 1–23. doi: 10.1080/14772019.2016.1228549

Pérez-García, A. (2018). New genera of Taphrosphyina (Pleurodira, Bothremydidae) for the French Maastrichtian '*Tretosternum*' *ambiguum* and the Peruvian Ypresian '*Podocnemis*' *olssoni*. *Hist. Biol.* 30, 1–6. doi: 10.1080/08912963.2018.1506779

Pérez-García, A. (2019). A new member of Taphrosphyini (Pleurodira, Bothremydidae) from the Maastrichtian of Niger. *J. Afr. Earth. Sci.* 158, 103548. doi: 10.1016/j.jafrearsci.2019.103548

Pérez-García, A. (2023). The ornamented shell of a new bothremydid turtle from the Uppermost Cretaceous of Niger. *Diversity* 15, 375. doi: 10.3390/d15030375

Pérez-García, A., Ortega, F., and Murelaga, X. (2012). A new genus of Bothremydidae (Chelonii, Pleurodira) in the Cretaceous of Southwestern Europe. *Geobios* 45, 219–229. doi: 10.1016/j.geobios.2011.03.001

Rollot, Y., Evers, S. W., and Joyce, W. G. (2021). A review of the carotid artery and facial nerve canal systems in extant turtles. *PeerJ* 8, e10475. doi: 10.7717/peerj.10475

Schmidt, K. P. (1940). A new turtle of the genus *Podocnemis* from the cretaceous of Arkansas. *Field Mus. Nat. Hist. Geol.* 8, 1–12. doi: 10.5962/bhl.title.3424

Schmidt-Nielsen, K., and Fange, R. (1958). Salt glands in marine reptiles. *Nature* 182, 783–785. doi: 10.1038/182783a0

Schwenk, K. (2008). "Comparative anatomy and physiology of chemical senses in nonavian aquatic reptiles," in *Sensory Evolution on the Threshold, Adaptations in Secondarily Aquatic Vertebrates*. Eds. J. G. M. Thewissen and S. Nummels (Berkeley: University of California Press), 65–81.

Tada, S., Tsuihiji, T., Morgan, D. J., Witmer, L. M., and Werneburg, I. (2025). Evolution of the rostral vasculature in turtles. *Swiss J. Palaeontol.* 144, 64. doi: 10.1186/s13358-025-00403-3

Werneburg, I., Evers, S. W., and Ferreira, G. S. (2021). On the "cartilaginous rider" in the endocasts of turtle brain cavities. *Vert. Zool.* 71, 403–418. doi: 10.3897/vz.71.e66756

Werneburg, I., Wilson, L. A. B., Parr, W. C. H., and Joyce, W. G. (2015). Evolution of neck vertebral shape and neck retraction at the transition to modern turtles: an integrated geometric morphometric approach. *Syst. Biol.* 64, 187–204. doi: 10.1093/sysbio/syu072

Wyneken, J. (2001). *The Anatomy of Sea Turtles* Vol. 470 (Miami (USA: U.S. Department of Commerce NOAA Technical Memorandum), 1–172.

Yoshida, M., Motokawa, M., and Endo, H. (2022). Osteological and vascular morphology and electrolyte homeostasis of sea turtles. *J. Vet. Med. Sci.* 84, 1001–1009. doi: 10.1292/jvms.21-0624